**Supporting Information**

# Molecular determinants conferring the stoichiometric-dependent activity of α-conotoxins at the human α9α10 nicotinic acetylcholine receptor subtype

Rilei Yu[1,3†*], Han-Shen Tae[2†], Nargis Tabassum[1,3], Juan Shi [1,3], Tao Jiang[1,3] and David J. Adams[2*]

[1]*Key Laboratory of Marine Drugs, Chinese Ministry of Education, School of Medicine and Pharmacy, Ocean University of China, Qingdao 266003, China*
[2]*Illawarra Health and Medical Research Institute (IHMRI), University of Wollongong, Wollongong, New South Wales 2522, Australia*
[3]*Laboratory for Marine Drugs and Bioproducts of Qingdao National Laboratory for Marine Science and Technology, Qingdao 266003, China*

**Contents of S1**

**Homology modeling**

The extracellular domain sequence of the hα1, α3, α4, α6, α7, α9, and α10 nAChR subunits were retrieved from the Uniprot database.[1] Both crystal structures of *Aplysia californica* AChBP (acetylcholine binding protein) in complex with α-conotoxin PnIA[A10L,D14K] (PDB code 2BR8), and the hα9 nAChR subunit extracellular domain (PDB code 4D01) from the Protein Data Bank, were used as templates to build 200 models of each α-conotoxin–nAChR complexes.[2,3] Models with the lowest DOPE score were selected for further structural refinement using molecular dynamics (MD) simulations. The structures of Vc1.1 analogues, Vc1.1[D11N] and Vc1.1[PeIA], were generated using Modeller based on the NMR structure of Vc1.1(PDB code 2H8S).[4]

**Molecular dynamics simulations**

The protonation states of His, Asp and Glu residues at the conotoxin/nAChR complexes were predicted using the PropKa 3.1 method.[5] The receptor complexes were solvated in a truncated octahedral TIP3P water box containing ~10800 water molecules. Sodium ions were added to neutralize the systems. The systems were first minimized with 3,000 steps of steepest descent and then 3,000 steps of conjugate gradient with the solute restrained to their position by a harmonic force of 100 kcal/mol·Å$^2$. A second minimization was then performed but with all position restraints withdrawn. The systems were then gradually heated up from 50 to 300 K in the NVT ensemble over 100 ps with the solute restrained to their position using a 5 kal/mol·Å$^2$ harmonic force potential. MD simulations were then carried out in the NPT ensemble, and the position restraints were gradually removed over 100 ps. The production runs were conducted over 50 ns simulation time with pressure coupling set at 1 atm and a constant temperature of 300 K. The MD simulations used a time step of 2 fs and, all bonds involving hydrogen atoms were maintained to their standard length using the SHAKE algorithm.[6] The particle-mesh Ewald (PME) method was used to model long-range electrostatic interactions.[7] MD trajectories were analyzed using VMD (http://www.ks.uiuc.edu/) and molecules were drawn using PyMol (Schrödinger, LLC).

For validation of the Vc1.1 analogue stability, 100 ns repeated MD simulations were performed on Vc1.1[N9D] and Vc1.1[PeIA] systems respectively, using the same method as described above.

**Binding energy decomposition**

To quantify the binding energy contribution of these key residues in the ligand binding site, binding energy decomposition was carried out using the MMPBSA.py script in AMBER16.[8] The binding free energy ($\Delta G_{binding}$) values were calculated using the following equation:

$$\Delta G_{binding} = G_{complex} - G_{ligand} - G_{receptor} \quad (1)$$

where the binding free energy ($\Delta G_{binding}$) was determined using MMGB/SA method.[9] This method was identified in our previous study as being slightly more efficient for ranking mutational energies based on homology models than the MMPB/SA method. Details of the MMGB/SA method on peptide binding energy calculation was described in our previous modelling studies.[10]

**Peptide synthesis**

Briefly, Vc1.1[D11N] and Vc1.1[PeIA] were assembled on rink amide methylbenzhydrylamine resin (Novabiochem) using solid-phase peptide synthesis with a neutralization/2-(1H-benzotriazol-1-yl)-1,1,3,3-tetramethyluronium hexafluorophosphate activation procedure for Fmoc (*N*-(9-fluorenyl)methoxycarbonyl) chemistry. Cleavage was achieved by treatment with 88:5:5:2 ratio of trifluoroacetic acid (TFA), phenol, water and triisopropylsilane as scavengers, at room temperature (20−25 °C) for 2 h. TFA was evaporated at low pressure in a rotary evaporator. Peptides were precipitated with ice-cold ether, filtered, dissolved in 50% buffer A/B (buffer A consists of 99.95% $H_2O$/ 0.05% TFA and buffer B consists of 90% $CH_3CN$/10% $H_2O$/0.045% TFA), and lyophilized. Crude peptides were purified by RP-HPLC on a Phenomenex $C_{18}$ column, and its molecular mass was confirmed using electrospray mass spectrometry before they were pooled and lyophilized for oxidation. The four cystines in the peptides were selectively oxidized in two steps. In the first step the non-protected cystines were oxidized in 0.1 M $NH_4HCO_3$ (pH 8–8.5) at a concentration of 0.5 mg/ml, and stirred at room temperature overnight. In the second step, the Acm-protected cystines were oxidized by dissolving the peptides in iodine solution filled at concentration of 1 mg/ml, and stirred for 30 min. Ascorbic acid was then added to stop the oxidizing reaction and the solution was stirred again until no colour was visible. After two rounds of oxidation, peptides were purified by RP-HPLC and their mass (Figure S7) and purity (Figure S8) were validated using electrospray-mass spectrometry (MS) and analytical RP-HPLC, respectively.

**Circular dichroism (CD) study**

CD spectra were performed on Jasco J-810 spectropolarimeter over the wavelength range of 250-190 nm using a 1.0 mm path length cell, a bandwidth of 1.0 nm, a response time of 2 s, and averaging over three scans. Spectra were recorded at room temperature under nitrogen atmosphere. Peptides were dissolved in buffer A and buffer B. The concentration of Vc1.1, Vc1.1[D11N], Vc1.1[PeIA], and PeIA was 0.28 mM, 0.28 mM, 0.29 mM and 0.30 mM, respectively. The spectra are expressed as molar ellipticity $([\theta])\cdot[\theta] = 1000\cdot mdeg/(l\cdot c)$ where, mdeg is the raw CD data, c is the peptide molar concentration (mM), and l is cell path length (mm).

**Oocyte preparation and microinjection**

All procedures were approved by the University of Sydney Animal Ethics Committee (project number 2016/970). Stage V-VI oocytes (Dumont's classification; 1200-1300 μm diameter) were obtained from *Xenopus laevis*, defolliculated with 1.5 mg/ml collagenase Type II (Worthington Biochemical Corp., Lakewood, NJ) at room temperature for 1-2 h in OR-2 solution containing (in mM) 82.5 NaCl, 2 KCl, 1 $MgCl_2$ and 5 HEPES at pH 7.4. Oocytes were injected with 35 ng cRNA for hα9α10 nAChR (concentration confirmed spectrophotometrically and by gel electrophoresis) at α9:α10 subunit mRNA ratios of 1:1. 1:3 and 3:1, using glass pipettes pulled from glass capillaries (3-000-203 GX, Drummond Scientific Co., Broomall, PA, USA). Oocytes were incubated at 18 ºC in sterile ND96 solution composed of (in mM) 96 NaCl, 2 KCl, 1 $CaCl_2$, 1 $MgCl_2$ and 5 HEPES at pH 7.4, supplemented with 5% FBS, 50 mg/L gentamicin (GIBCO, Grand Island, NY, USA) and 10000 U/mL

penicillin-streptomycin (GIBCO, Grand Island, NY, USA).

**Oocyte two-electrode voltage clamp recording and data analysis**

Voltage-recording and current-injecting electrodes were pulled from GC150T-7.5 borosilicate glass (Harvard Apparatus, Holliston, MA) and filled with 3 M KCl giving resistances of 0.3–1 MΩ.

Oocytes were incubated in 100 µM BAPTA-AM ~3 h before recording and perfused with ND115 solution containing (in mM): 115 NaCl, 2.5 KCl, 1.8 $CaCl_2$, and 10 HEPES at pH 7.4 using a continuous Legato 270 push/pull syringe pump perfusion system (KD Scientific, Holliston, MA, USA) at a rate of 2 mL/min in an OPC-1 perfusion chamber of < 20 µL volume (Automate Scientific, Berkeley, CA, USA). Due to the $Ca^{2+}$ permeability of hα9α10 nAChRs, BAPTA-AM incubation was carried out to prevent the activation of *X. laevis* oocyte endogenous $Ca^{2+}$-activated chloride channels.

Initially, oocytes were briefly washed with ND115 solution followed by 3 applications of acetylcholine (ACh) at a half-maximal excitatory ACh concentration ($EC_{50}$) for hα9α10 nAChRs. Washout with bath solution was done for 3 min between ACh applications. Oocytes were incubated with peptides for 5 min with the perfusion system turned off, followed by co-application of ACh and peptide with flowing bath solution. All peptide solutions were prepared in ND115 + 0.1 % bovine serum albumin. Peak current amplitudes before (ACh alone) and after (ACh + peptide) peptide incubation were measured using Clampfit version 10.7.0.3 software (Molecular Devices, Sunnyvale, CA, USA), where the ratio of ACh + peptide-evoked current amplitude to ACh alone-evoked current amplitude was used to assess the activity of the peptides at hα9α10 nAChRs. All electrophysiological data were pooled (n = 3-16) and represent means ± standard error of the mean (SEM). Data analysis was performed using GraphPad Prism 5 (GraphPad Software, La Jolla, CA, USA). ACh $EC_{50}$ and α-conotoxin $IC_{50}$ values were determined from concentration-response relationships fitted to a non-linear regression function and reported with error of the fit. Data sets were compared using Tukey's test. Differences were regarded statistically significant when $p < 0.05$.

## REFERENCES


(1) Magrane, M.; UniProt Consortium. UniProt Knowledgebase: A Hub of Integrated Protein Data. *Database J. Biol. Databases Curation* **2011**, *2011*, bar009.

(2) Zouridakis, M.; Giastas, P.; Zarkadas, E.; Chroni-Tzartou, D.; Bregestovski, P.; Tzartos, S. J. Crystal structures of free and antagonist-bound states of human α9 nicotinic receptor extracellular domain. *Nat. Struct. Mol. Biol.* **2014**, *21*, 976–980.

(3) Celie, P. H. N.; Kasheverov, I. E.; Mordvintsev, D. Y.; Hogg, R. C.; van Nierop, P.; van Elk, R.; van Rossum-Fikkert, S. E.; Zhmak, M. N.; Bertrand, D.; Tsetlin, V.; Sixma, T. K.; Smit, A. B. Crystal structure of nicotinic acetylcholine receptor homolog AChBP in complex with an α-conotoxin PnIA variant. *Nat. Struct. Mol. Biol.* **2005**, *12*, 582–588.

(4) Clark, R. J.; Fischer, H.; Nevin, S. T.; Adams, D. J.; Craik, D. J. The synthesis, structural characterization, and receptor specificity of the α-conotoxin Vc1.1. *J. Biol. Chem.* **2006**, *28*, 23254–23263.
(5) Olsson, M. H. M.; Søndergaard, C. R.; Rostkowski, M.; Jensen, J. H. PROPKA3: Consistent treatment of internal and surface residues in empirical pKa predictions. *J. Chem. Theory Comput.* **2011**, *7*, 525–537.
(6) Miyamoto, S.; Kollman, P. A. Settle: An analytical version of the SHAKE and RATTLE algorithm for rigid water models. *J. Comput. Chem.* **1992**, *13*, 952–962.
(7) Darden, T.; York, D.; Pedersen, L. Particle mesh Ewald: An N·log(N) method for Ewald sums in large systems. *J. Chem. Phys*. **1993**, *98*, 10089.
(8) Miller, B. R.; McGee, T. D.; Swails, J. M.; Homeyer, N.; Gohlke, H.; Roitberg, A. E. MMPBSA.Py: An efficient program for end-state free energy calculations. *J. Chem. Theory Comput.* **2012**, *8*, 3314–3321.
(9) Onufriev, A.; Bashford, D.; Case, D. A. Exploring protein native states and large-scale conformational changes with a modified generalized Born model. *Proteins* **2004**, *55*, 383–394.
(10) Yu, R.; Craik, D. J.; Kaas, Q. Blockade of neuronal α7-nAChR by α-conotoxin ImI explained by computational scanning and energy calculations. *PLoS Comput. Biol.* **2011**, *7*, e1002011.

**Table S1. Quantitative analysis of the purity of the peptide.**

| Name | Retention time (min) | Peak area | Total peak area | Purity |
|---|---|---|---|---|
| Vc1.1[D11N] | 21.773 | 2329446 | 2382506 | 97.8% |
| Vc1.1[PeIA] | 12.847 | 18474014 | 18791063 | 98.3% |
| PeIA | 23.307 | 4330976 | 4557830 | 95.0% |
| RgIA# | 15.860 | 4267319 | 4437735 | 96.16% |
| Vc1.1 | 22.053 | 2754800 | 2898800 | 95.03% |

The purity of the peptide was analysed using analytical RP-HPLC at a flow rate of 1 mL/min with the concentration of the buffer B increased from 5% to 100% with a time span of 50 min.

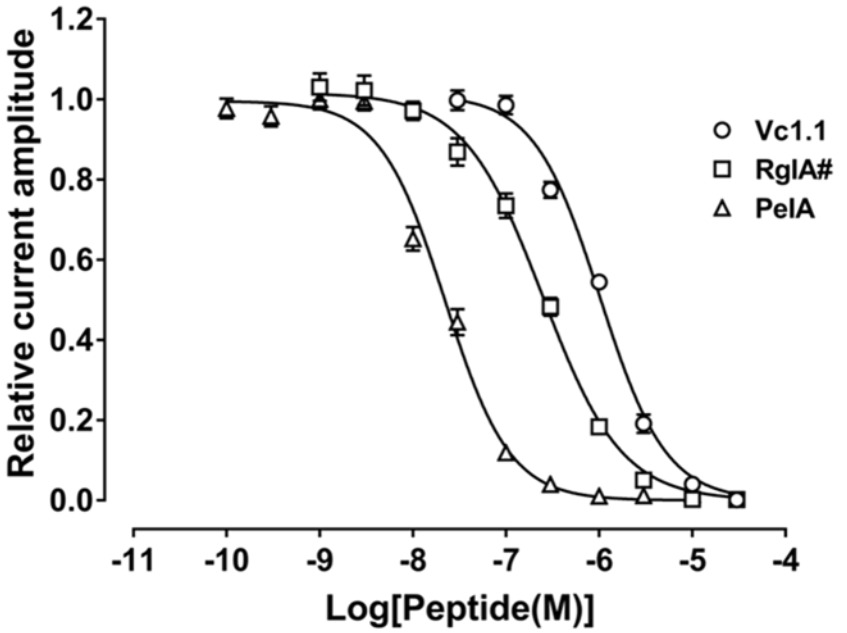


**Figure S1. Activity of the α-conotoxins Vc1.1, RgIA#, and PeIA at the human α9α10 nAChR**. Concentration-response relationships of relative ACh-evoked current amplitude mediated by hα9α10 nAChR at hα9 to hα10 subunit 1:1 ratio in the presence of Vc1.1, PeIA, and RgIA# (0.1 nM – 30 μM) giving $IC_{50}$ values of 1.0 ± 0.1 μM, 22.2 ± 1.6 nM and 248.7 ± 19.2 nM, respectively (mean ± SEM, n = 5-16). Whole-cell hα9α10 nAChR-mediated currents were activated by 6 μM ACh.

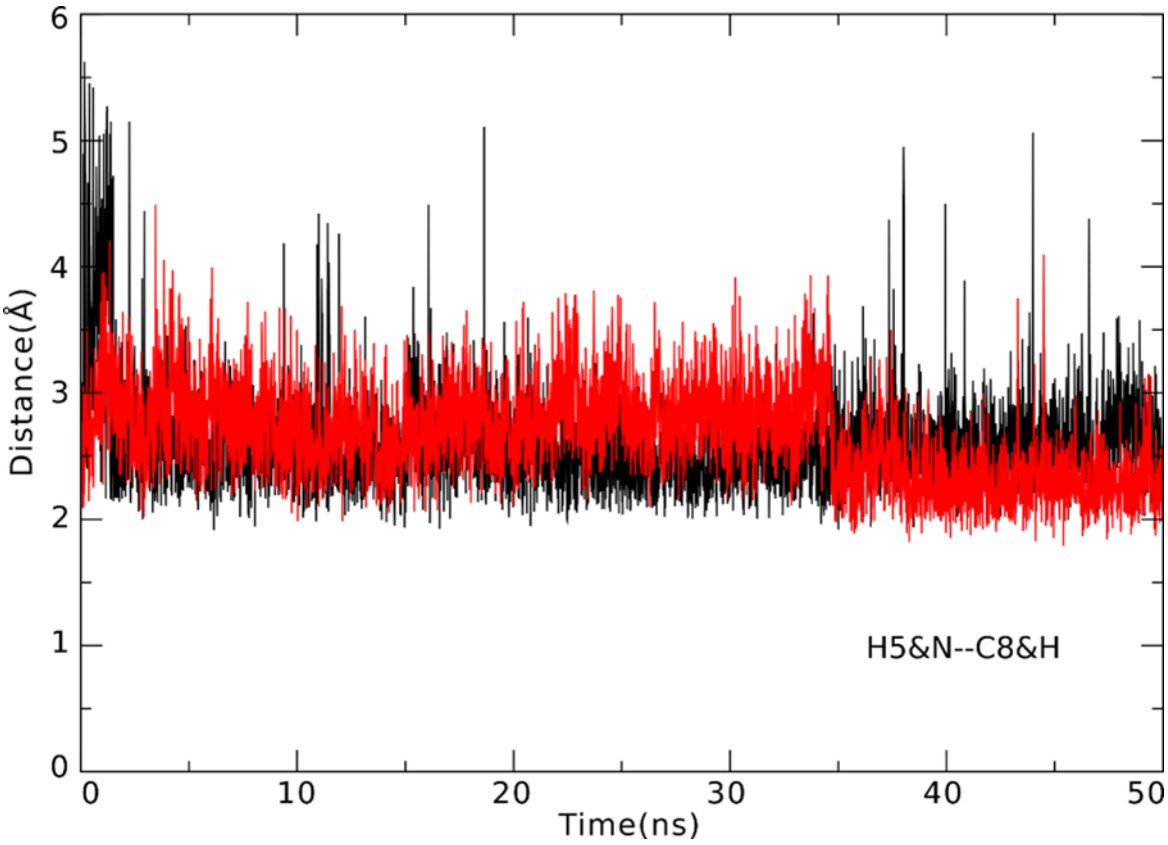


**Figure S2. Internal backbone H-bond between PeIA residues H5 and C8**. Stability in the distance between N atom of His5 and H atom of Cys8 (H5&N—C8&H) in PeIA at the α10(+)α9(–) (red) and α9(+)α9(–) (black) binding sites.

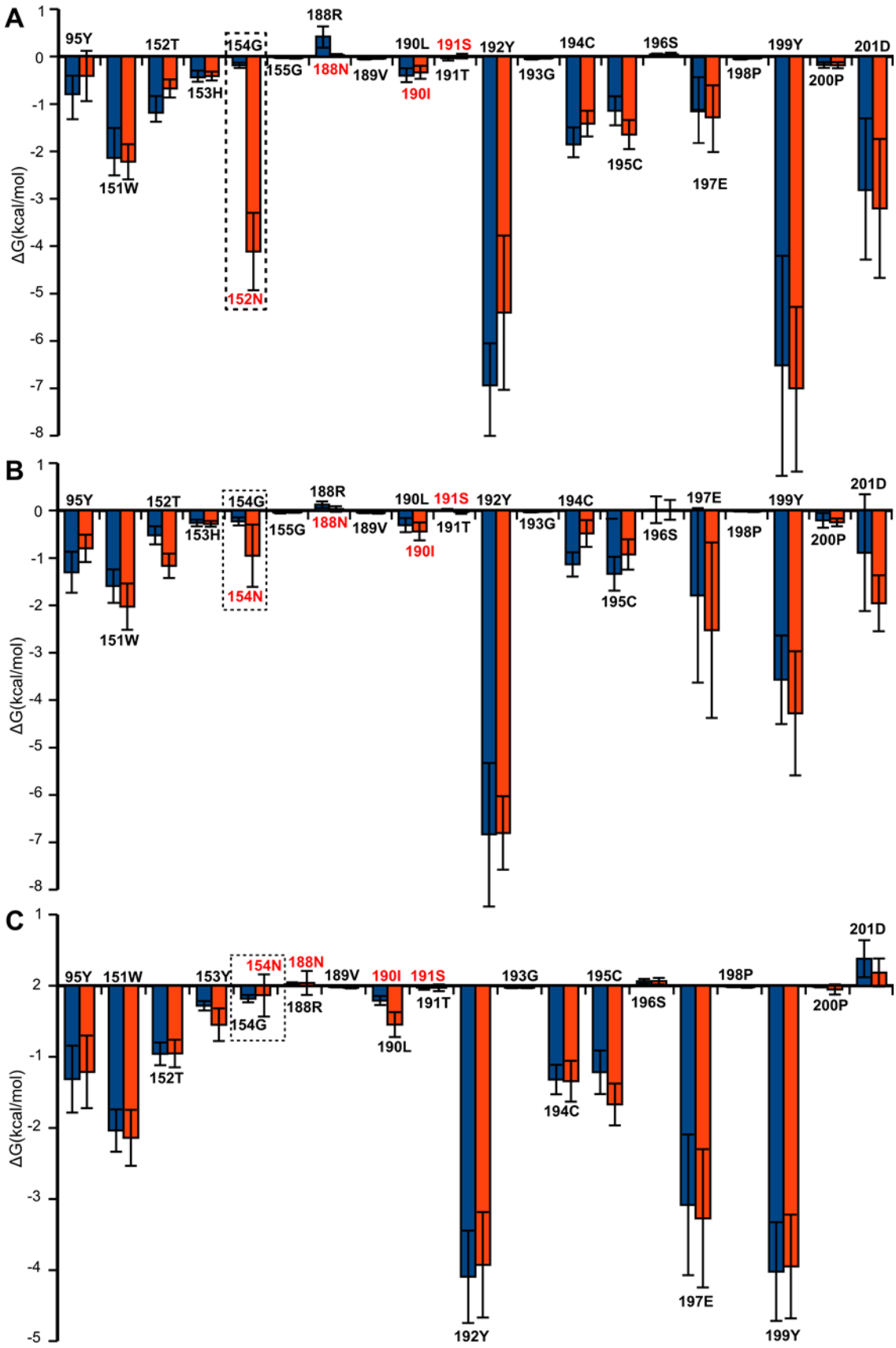


**Figure S3. Side chain energetic contribution to the α-conotoxin's binding affinity.**

**(**A-C) Side chain-energetic contribution for residues at the principal components of

the α10(+)-α9(–) (blue) and α9(+)-α9(–) (red) interfaces to the binding affinity of Vc1.1, RgIA#, and PeIA, respectively. Non-conserved residues from the α9 subunit are labelled red. Side chain energetic contribution of the α9 and α10 subunit residues at position 154 is highlighted (dashed frame).

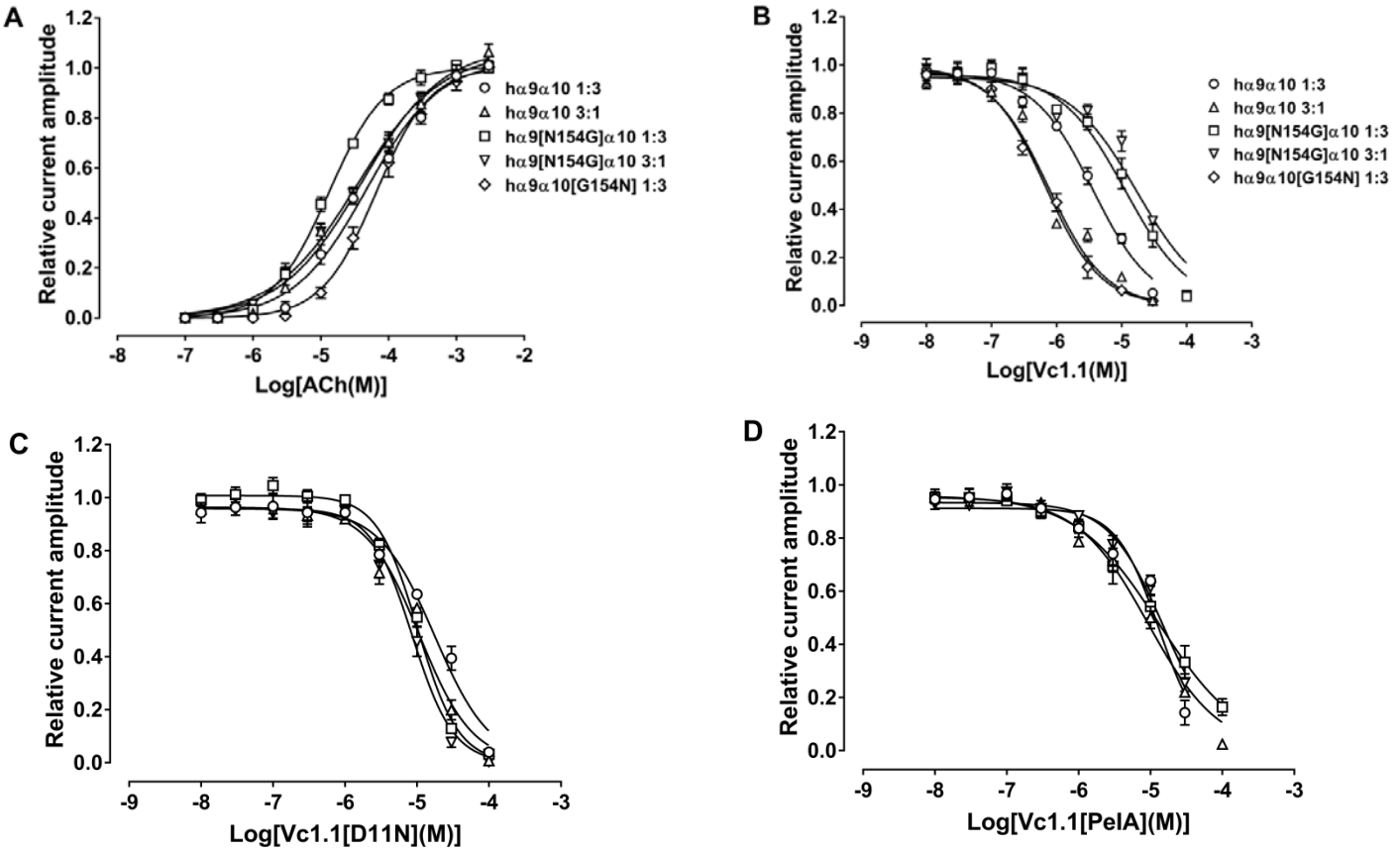


**Figure S4. Activity of α-conotoxins at human α9α10 and α9[N154G]α10 nAChRs expressed from varied α9:α10 mRNA ratios**. (A) ACh concentration-response relationship obtained for relative ACh-evoked current amplitude mediated by hα9α10 nAChRs (mean ± SEM, n = 3-6) at varying hα9 to hα10 subunit ratios. $EC_{50}$ values are given in Table 1. Concentration-response relationships for the inhibition of relative ACh-evoked current amplitude mediated by hα9α10 nAChRs (mean ± SEM, n = 3-16) at varying hα9 to hα10 subunit ratios in the presence of (B) Vc1.1, (C) Vc1.1[D11N], and (D) Vc1.1[PeIA]. $IC_{50}$ values are given in Table 1. Whole-cell hα9α10 nAChR-mediated currents at 1:3 and 3:1 ratios were activated by 50 μM and 30 μM ACh, respectively, whole-cell hα9[N154G]α10 nAChR-mediated currents at 1:3 and 3:1 ratios were activated by 20 μM and 30 μM ACh, respectively and whole-cell hα9α10[G154N] nAChR-mediated currents at 1:3 ratios were activated by 60 μM ACh (close to their respective $EC_{50}$ values).

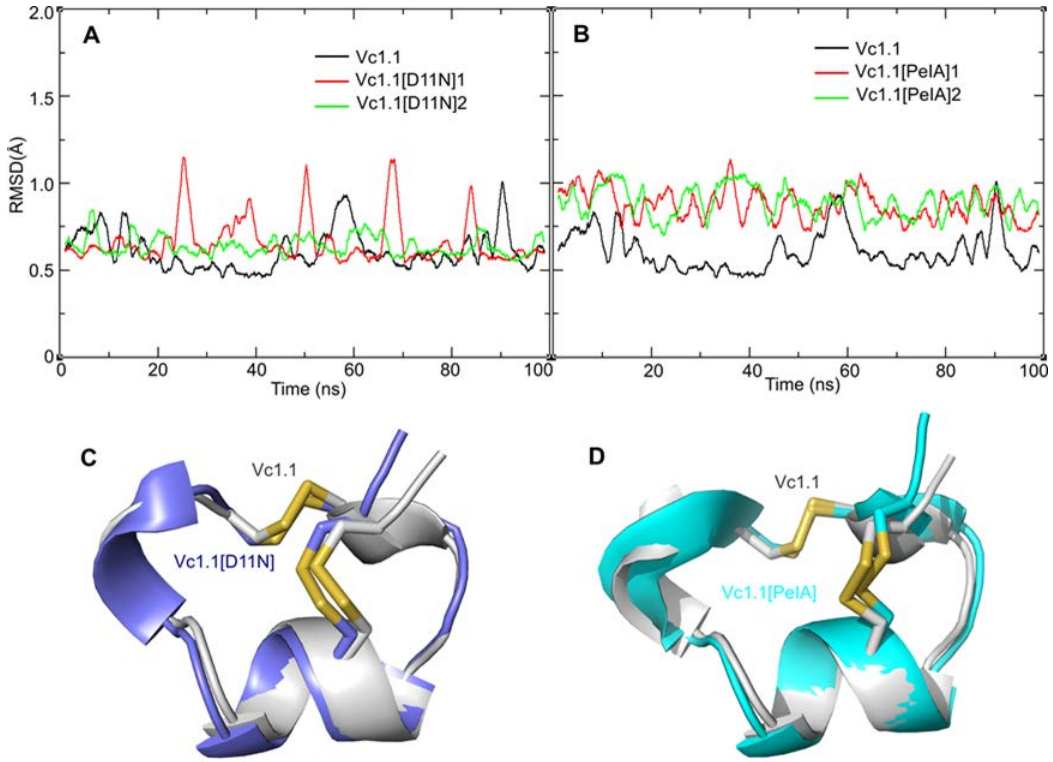


**Figure S5. Structural comparison of wild-type Vc1.1 and analogues Vc1.1[D11N] and Vc1.1[PeIA]**. RMSD (root mean square deviation) for the backbone atoms of (A) Vc1.1 (black) vs Vc1.1[D11N] (red and green), and (B) Vc1.1 vs Vc1.1[PeIA] (red and green). Structural comparison of (C) Vc1.1 (grey) vs Vc1.1[D11N] (blue), and (D) Vc1.1 (grey) vs Vc1.1[PeIA] (cyan). The disulfide bonds are coloured yellow.

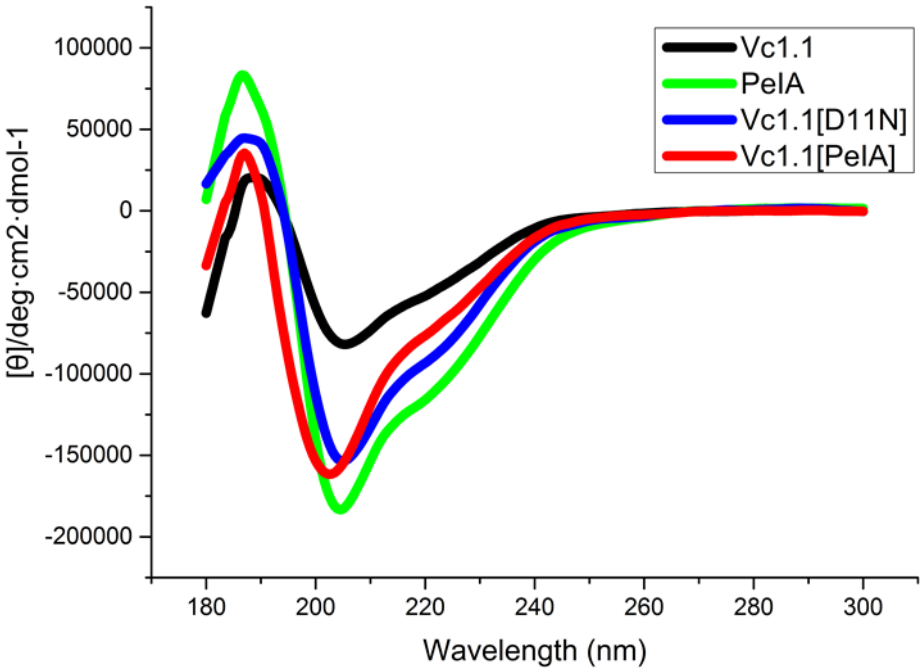


**Figure S6. Spectroscopic comparison of wild-type Vc1.1 and analogues Vc1.1[D11N] and Vc1.1[PeIA].** Circular dichroism spectra of Vc1.1 (black), Vc1.1[D11N] (blue), and Vc1.1[PeIA] (red).

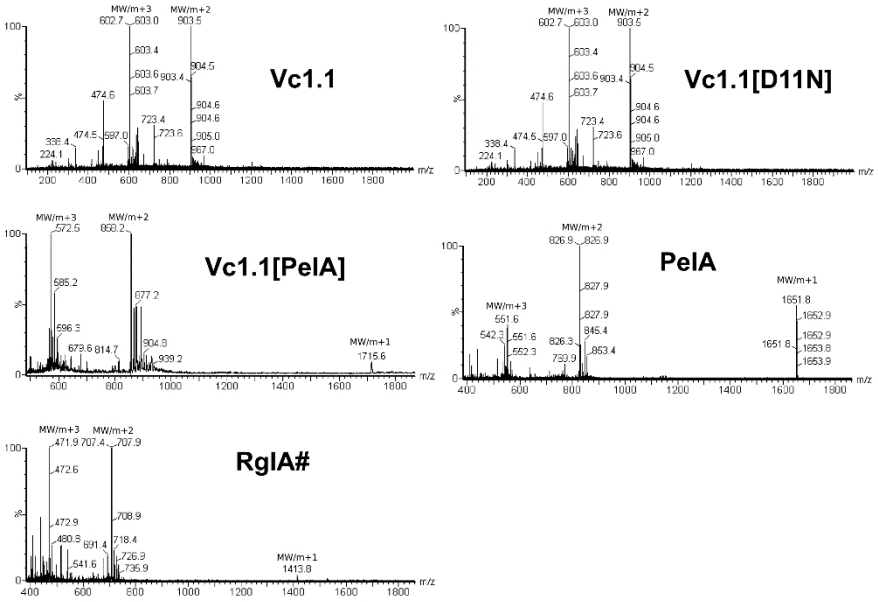


**Figure S7. MS spectra of Vc1.1, Vc1.1[D11N], Vc1.1[PeIA], PeIA, and RgIA#**.

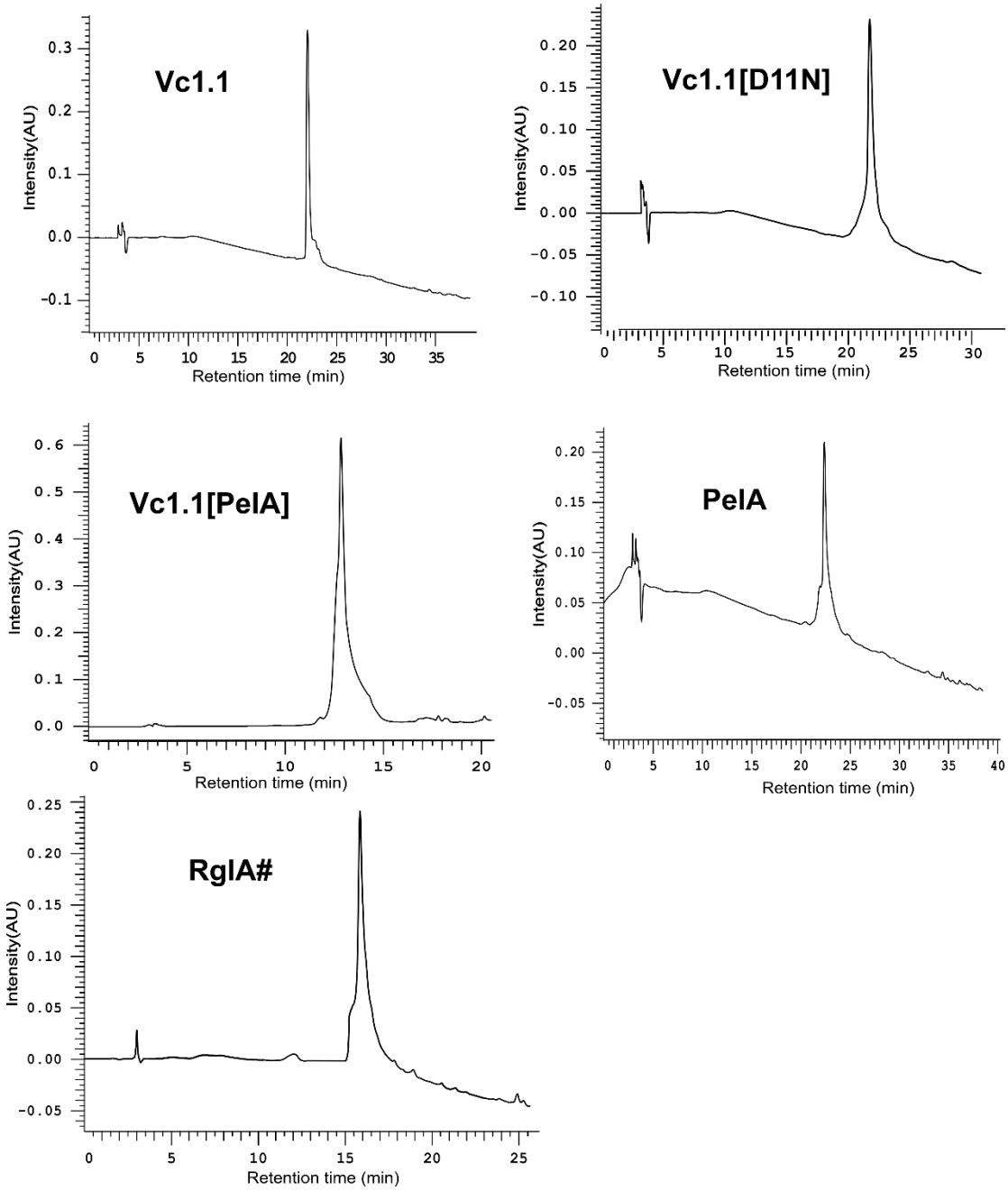


**Figure S8. Analytical RP-HPLC profiles of Vc1.1, Vc1.1[D11N], Vc1.1[PeIA], PeIA, and RgIA#.**